Development of a squirrel-inspired passive latching system to quickly attach to tree surfaces using bistable structures with tunable activation energies.

Kabir Knupp[1], Thrishantha Nanayakkara[2]

Abstract*— Amazonian rainforests remain unexplored, but reaching and staying in the canopy is energy intensive. Moving between trees is even more difficult; for a robot to glide through the air and make a stable vertical landing, it must be able to grab the attachment surface as soon as it makes contact, or it could bounce from it. This paper presents a novel concept for rapid, lightweight, motorless surface latching onto trees using bistable strips as clawed finger units, secured by a tightenable bolt. The bolt decreases the energy needed for buckling and allows the finger to be deployed by a tunable amount of contact force with the surface. Three simple experiments were conducted to understand how changing the geometry of the bistable strip affects its grip and retraction force. The results showed that the strip's surface area relates to its embodied elastic energy, and that a tapered bistable strip reduces the retraction force required when being pulled from the thin end. Two types of thin PLA 'gloves' with different anchors at the tip were designed to test the performance of the finger unit: one with two rigid fishing hooks and another with multiple semi-compliant steel spikes. Experimental results show that both claws successfully attach to a range of tree surfaces, but the fishing hooks can carry much greater payloads. The system is tested through its integration into an underactuated tree-climbing robot with two limbs. The robot lacked the degrees of freedom needed to maneuver complex tree environments, but was able to stay suspended with one arm and steadily lift the other, demonstrating the latching claw's ability to generate adhesive forces. *Design Build & Test, 5456 words.

I. INTRODUCTION

Rainforest preservation is crucial to sustainable growth. 25% of pharmaceuticals come from there [1], and only 36% of the world's tropical rainforests remain in tact today [2]. Leading causes of deforestation are the clearing of forestland for farming [3] but commercialisation of non-timber forest products (NTFP) could incentivise governments to protect the rainforest if they attracted more wealth [4].

Establishing alternate value streams from the rainforest is key. Rare fungi that have high medicinal value grow in the upper canopies, but NTFP needn't be physical. The rainforest also contains non-tangible commodities that are valued by the west, such as the immersive sounds of ecosystems.

For humans, reaching the canopy to monitor these resources is difficult; rope access techniques must be deployed and bridges installed. Unmanned aerial vehicles can ascend relatively fast but have limited flight time. An energy efficient tree-climbing and perching robot, that can traverse the forest and collect data/sense the location of NTFP is most desirable for this application. To traverse the rainforest, the robot should be able to glide between trees and therefore needs to be very light. The rainforest is an unpredictable environment, and the robot won't always have time to prepare before attaching to a new tree, the reaction time for grasping must therefore be instantaneous. The robotic systems presented in this paper were designed to be cheap to manufacture, use standardised components, and be made from waste materials so that local rainforest communities can assist with their repair.

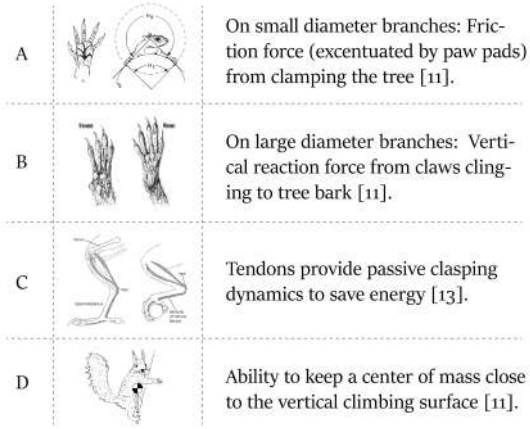

Fig. 1: Four key biological adaptations for mammalian and avian tree climbing.

A. General Robotic Solutions

Existing tree-climbing robots attach to tree surfaces using either of two main methods:

1) Enclosing the diameter of the tree as if it were a large cylinder [5] [6] [7], but this constrains the size of climbable trees.
2) Infiltrating the tree's wood with sharp needles [8] [9]. This requires substantial motors, diminishing the robot's potential ability to float between trees.

A robot for the proposed application should stay suspended in the canopy for long periods of time; and thus benefits from static gripping with zero energy consumption when perched on the tree. Treebot, the most popular tree-climbing robot in the literature, achieves this through the use of preloaded springs [10].

[1]S. Kabir Knupp is with the Dyson School of Design Engineering, Imperial College London, London, SW7 2AZ (email: kabir.knupp18@imperial.ac.uk) (email: patrick.mcguckian18@imperial.ac.uk)

[2]N. Thrishantha Nannayakara is with Dyson School of Design Engineering, Imperial College London, London, SW7 2AZ (email: Team member-3@gmail.com)

B. Biological Inspirations

Figure 1 summarises fundamental biological adaptations found in mammals and birds that assist with climbing trees. Tree-climbing mammals can reach around branches of smaller diameter and use the force of friction to stay suspended. The condition $Fr > mg$ ($Fr = \mu L$) must be satisfied, where L is the opposing normal force that paws apply to the tree surface. Row B depicts the method used when tree branches with diameter wider than the rodent's reach cause it to lay flatter and unable to provide the inward pushing force L that provides the friction to resist gravity [11]. The rodent must then rely on the claws on its hands and feet to dig into the substrate as anchor points. Interlocking the surface of the mammal with that of the support generates a new contact surface that is perpendicular to the pulling force of gravity [12]. Parameters that affect gripping ability are the claws' curvature and the depth to which they will penetrate [11].

Bird talons are similar in principle but have an additional system of tendons that cause their feet to passively clasp as their knee joints bend, and that motion cannot be undone until their legs straighten again [12].

C. Bio-inspired robotic solutions

Much research in recent years has focused on letting drones perch to recover battery life. Biomimetic mechanisms inspired by bird legs and feet (as shown in row C of figure 1) have been imitated to transform impact energy into grasping force, and let drones perch on complex horizontal surfaces such as tree branches [13]. Airborne robots that are capable of perching on vertical surfaces are also a hot research topic; many of which achieve suspension by forcing opposing miniature spines that catch onto surface asperities [14] [15] [16]. Perching drones like Stanford's SCAMP robot fly towards a vertical urban surface such as a wall and bump their tail into it, which acts as a pivot point [17]. They then use their rotors' thrust to flip over and push themselves into the wall, giving them time to engage their microspines and stay suspended.

D. Technology Gap

The robots described above are sophisticated but take a considerable time to engage the latching mechanism and depend on sensory feedback. There are few robotic technologies designed to cope with the irregularities of natural environments. Here we present the journey towards a technology for latching to vertical surfaces, which uses bistable structures with tuneable activation energy for instant motorless latching. As can be seen in figure 2, bistable structures have two stable mechanical shapes [18], which often have two different curvature axes. Slap bracelets, originally under the brand name of "Slap Wraps", are a renowned example of bistable structures. They are a long rectangular strip of flexible stainless steel sheathed with a silicone cover, and can be activated (switch stability modes) using mechanical force [19]. The series of designs communicated in this paper allow the system to be conveniently adjusted so that a range

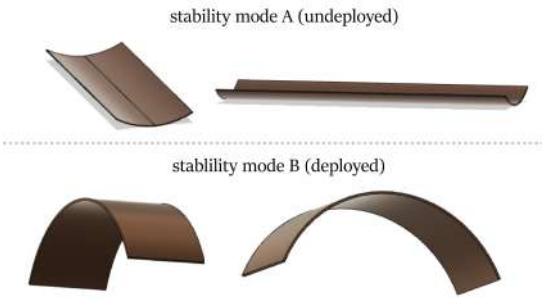

Fig. 2: Bistable structures labelled with two stability modes of different curvature axes.

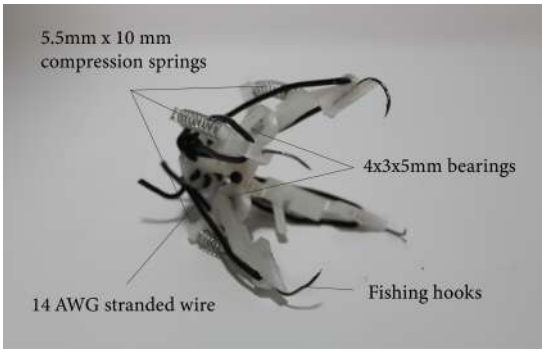

Fig. 3: Initial spring-loaded claw design for static gripping.

of desired activation force magnitudes between the fingers of each claw and the contact surface can be set manually. Bistable structures are advantageous for latching applications because of their very quick transition between bi-stable states, abundant fatigue life, and embodied elasticity. The system's response to sudden changes in force is instant and there is no reliance on sensory feedback for actuation. The work presented aims to further research on embodied perching methods onto ragged non-horizontal surfaces. The surface latching claw designs are developed through their integration into a tree climbing robot, whose climbing ability is tested. A series of simple experiments were then conducted to understand the relationship of various parameters within the latching claw design.

II. MECHANICAL DESIGNS & PROCESSES

Problem Statement: *Develop a passively latching claw, that is non-reliant on sensory feedback, and can quickly and firmly attach to tree surfaces upon making contact.*

A. Antecedent Latching Claw Design (spring-loaded fingers)

The gripper reviewed in this subsection is spring-loaded and was designed prior to that which uses bistable structures for each finger unit, but serves as a useful comparison. It consists of four 5.5mm x 10 mm compression springs, each acting upon a 3D printed (polylactic acid) finger unit press fitted to a 3x8x4mm ball bearing. Long nose pliers were used to decrease the curvature of carbon steel circle fishing hooks. One hook was melted into the end of each finger unit, leaving

Fig. 4: Spring-loaded claw payload testing with 250g at $\angle > 90°$

the angle between the finger and the spine of the hook at 90° (accurate to the nearest 5°). The barb of the hook was squashed to decomplicate the retraction of the spine from the tree. The claw performed well on a variety of trees and was able to support payloads of >200g at several attachment angles. The combined compression force generated by the four springs caused the spines to shallowly penetrate the surface of the bark. Unlatching the claw required 5.4N of force (measured by hanging weight from the bottom). The basic design successfully achieved static gripping with no energy consumption when attached to the tree and was able to suspend 400g of weight with ease.

Figure 5 shows two mechanisms that were investigated to keep the gripper open until contact force causes it to latch. The first involved a 3D printed cam mechanism inspired by those found in retractable click pens. The mechanism worked in principle, but was difficult to reset as there was excessive friction between the cam curve slot and the work part; expensive manufacture methods are required to produce a version that slides smoothly. The second mechanism aimed to retract a sliding cylinder cover that was connected to the bottom section of each finger (compressing the four springs) and offsetting it slightly to halt at the top of the shaft. As the claw experiences some force, the cylindrical cover realigns with the internal shaft and slides down freely, releasing the elastic energy stored by the springs and subsequently latching. The limitation of this mechanism is that the magnitude of force needed to re-align the shaft varies depending on its direction. Resetting the mechanism to put the claw in the unlatched state also demands a complex motion which is difficult to achieve with actuators and would require additional mechanisms to work reliably.

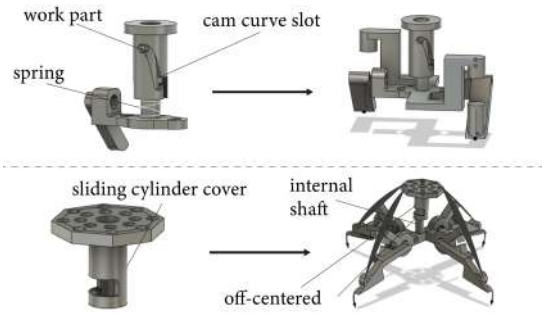

Fig. 5: Force activated latching mechanism designs that were considered: *a)* click pen inspired cam mechanism *b)* off-centered shaft cover.

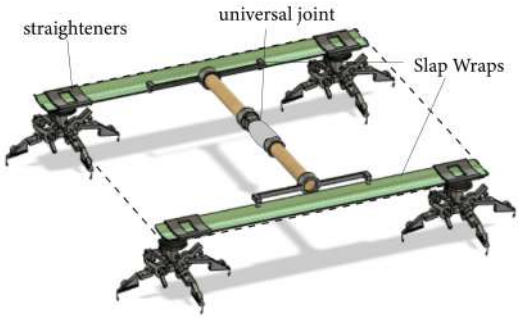

Fig. 6: Considered gliding body design with a bistable frame/skeleton.

Figure 6 illustrates a potential robot body design based on this latching claw. Two full length Slap Wraps connect to create a frame for a gliding membrane to attach to. As the robot collides with the target tree, its kinetic energy would cause the body to change stability modes, and wrap around the target tree (subject to its diameter).

B. Revised Latching Claw Design (Bistable Finger Structures)

The motivation behind using bistable structures as the fingers of the latching device is their stability in two states. When the claw is drawn back, the bistable structure reverts to state A; which is confirmed by a clicking sound. The function of the mechanism in subsection II-A is embedded in the bistable material as there are two stable modes whose changeover is managed by mechanical force. The transition between state A and B is very sudden, which is favorable for airborne robots moving at high speeds that could bounce from the attachment surface straight after a collision. The flexible steel has high tensile strength and is very light (a section of area $0.002205m^2$ weighs just $1.05g$).

1) Embodied elastic energy parameters: It was observed that lots of force was required to reset the bistable structures from state B back to state A. By altering the geometry of the bistable strip while keeping it symmetrical, it was found possible to irreversibly tune the overall embodied energy and therefore ease of return to stability mode A. The affecting

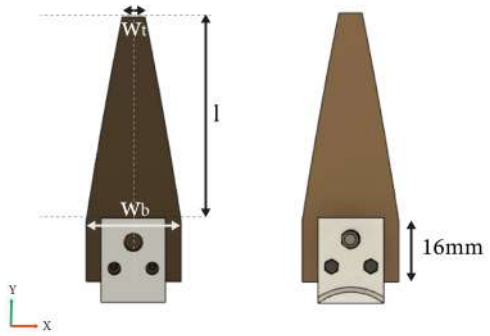

Fig. 7: Constant and variable parameters of the bistable finger.

Fig. 8: Initial bistable claw design - crossover mechanism deployed by pushing into the steel concave.

parameters, depicted in figure 7, were hypothesised to be width at the base w_b (relating to curvature of the concave), length l, and the width at the tip w_t. It was noticed that cutting a tapered petal-like shape makes the steel structure easier to reset. This relationship was explored experimentally and is recounted in section III-A.

2) Overlapping Structures: The headmost method for employing bistable structures as latching units was to overlap two bistable strips in a cross formation. As shown in figure 8, it was identified that sufficient pressure applied to the outside of the concave (to increase the radius of the curvature axis) initiates a transition to stablility state B. Based on this information, the bistable strip was sandwiched between two different objects. One small cylindrical object was placed at the bottom to apply upwards pressure to the concaves of the bistable strips, and a larger hollow cylindrical object on top to apply downward pressure to the top edges of the bistable strips when pressed, to change their curvature. The concept worked but a considerable push force of 4.9N (measured by loading weights and converting to newtons) was required to activate two 10mmx50mm overlapping bistable strips. The latching could only be initiated by high speed collisions with weight behind them due to the force required. The overlapping structures were also unable to interlock because of their changing shape and were able to move past each other; the design is therefore unsuitable for the desired application.

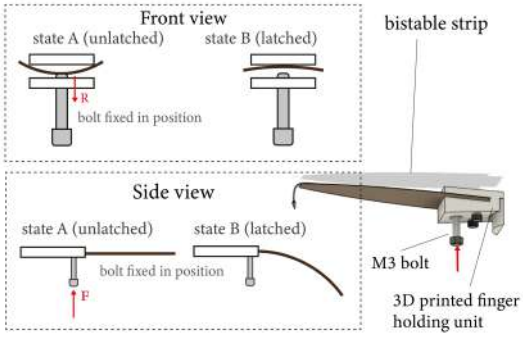

Fig. 9: Single bistable latching finger design and mechanism.

3) Single Finger: The next method was subject to the same principle as described in section II-B.2, but was more successful. A single bistable strip was wedged between a rigid 3D (PLA) printed top and bottom surface, with the concave facing downward. An M3 x 4mm x 5mm female knurled brass threaded insert was heated and fused centrally into the bottom of the component that holds the bistable strip. As illustrated in figure 9, a bolt was screwed into the threaded insert. the threaded insert keeps the bolt firmly in the position it was set to. Compliance in the 3d printed component means that abrupt force applied to the bottom of the bolt will initiate latching, as the bolt can push further into the concave, providing the needed activation energy. The system is tuned by tightening the bolt so that it is constantly applying a desired amount of pressure to the bottom of the bistable structure. The bolt's height can be adjusted through screwing or unscrewing to apply more or less force into the concave of the bistable strip respectively. This provides potential energy to the bistable structure, and keeps the bistable strip on the verge of switching states so that less energy needs to be given to the system to activate it. The design achieves a tunable state transition reactivity.

As the bistable strip moved in the enclosure, the system's reactivity would change as a result of displacement between the lowest point of the concave and the bolt. Two M3 holes with centers 10mm apart were consequently drilled into the bistable strip with a titanium drill bit and M2 bolts were used to fasten the bistable strip into the finger holding unit. There was no significant change in tuning over time after the strips had been fastened. As well as the variable tuning using pressure from the bolt, another method that was discovered to increase state-switching reactivity was to add weight to the end of the finger structure. The differences in moment of inertia across the bistable strip cause it to buckle into state B upon impact.

4) Entire Claw: The finger design was replicated four times and each one was interference fitted to surround a metal screw-on bottlecap, The bottle-cap was used because it is durable, lightweight, commonly available (as it has a standardised size), and permits each finger unit to be organised concentrically because it was been manufactured to be exactly circular. a 10mm$\pm$3mm diameter bamboo rod with a 4mm socket screw threaded insert in the base was

Fig. 10: Rapid iterations of the latching claw - to explore the effects of varying parameters.

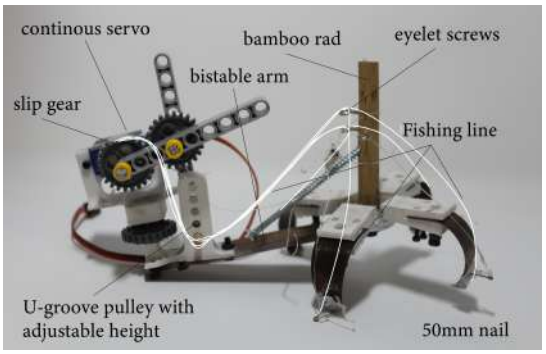

Fig. 11: Leg mechanism to retract or activate the bistable claw.

fastened to the center of the bottle cap using an m4 x 12mm bolt. Two 4mm nickel-plated eyelet screws were screwed at the top to guide 4 strands of 0.45mm monofilament fishing line that was later used to unlatch each finger unit. The height of the bamboo allowed the eyelet screws to guide the fishing line from a range of angles as if they were pulleys with some friction. The bamboo takes up little room, and is easily sourced. The fishing line was knotted to fishing hooks (glued to the tip of each finger) and acted as tendons to revert individual units from state B back to state A by contracting. This method of retraction was chosen because of its low energy in comparison to forcing the curvature axis back the other way. Unlike the spring loaded claw in section II-A, the mechanism of each finger unit is independent, meaning that each one can curl by different amounts, and those that don't receive sufficient activation energy upon contact won't deploy. With tree surfaces being lumpy and unpredictable, this could be advantageous in saving energy for the retraction.

C. Light Servo Retraction

The bistable steel used initially was taken from inside URAQT reflector strip snap bands. A $1.2kg/cm$ torque providing SG90 microservo (lightest easily accessible actuators on the marketplace) pulling 14mm from the center could revert two fingers of $l = 57mm$, $w_b = 18mm$ and $w_t = 8mm$, slotted 16mm deep into the finger holding unit. After changing to thinner steel found inside 'Cieex Slap Bands for Kids' which has thickness of 0.1mm compared to 0.2mm previously (measured with a digital vernier calliper of resolution ± 0.1), the microservo was able to retract four fingers of these dimensions.

D. Leg Mechanism

A leg mechanism was designed for the tree-climbing robot to peel back each of the four fingers completely and then buckle onto the next desired part of the tree surface, to let the fingers latch onto it. Figure 11 identifies the features of the leg mechanism.

A U624zz Carbon Steel Shell U-groove Pulley Roller Metal was used to guide the fishing line through a path that would create a kinetic chain to retract each finger, while bending the bistable arm back and storing the elastic potential energy needed to initiate buckling. The 30mm screw protruding from the bamboo was used to create a pivot point on the bistable arm, shifting the fulcrum from the base of the claw to the bottom of the arm, to make the kinetic links possible. The bistable arm was advantageous because it also switches stability mode upon buckling, and applies pressure into the surface of the tree, further keeping the claw from bouncing. Separate fishing line constrains the motion of the bi-stable arm.

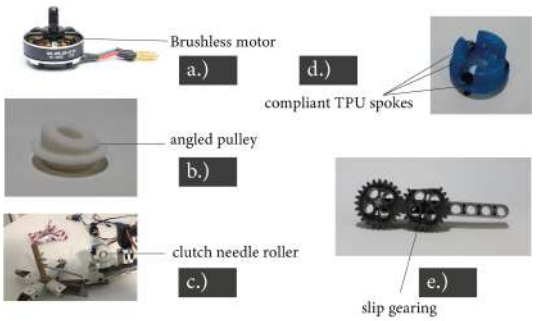

Fig. 12: Various buckling mechanism designs *a)*Brushless motor *b)* angled pulley *c)*Clutch bearing *d)*Compliant TPU spokes *e)* Slip gearing.

E. Release/activation mechanisms for buckling

The following research involved designing mechanisms that using just one actuator could slowly store up elastic potential energy in the four tendons and cause them to suddenly become slack to initiate buckling.

1) Brushless motor: This method involved winding up the tendons using a brushless motor. This method was limited, because although it is easy to release the string, the system could not be kept in a pulled back state. Brushless motors are also expensive for the application.

The rest of the methods described used an FS90R 360 Degree Continuous Rotation Micro Servo for its high torque:weight ratio, and easy bi-directional control (no motor drivers are required).

2) Angled pulley: This method involved drawing back the tendons on an angled pulley. The fishing line would slip

off after a certain number of rotations. The limitations of this method are its inconsistency and the tendon becomes contorted if it does not turn back the other way.

3) Clutch bearing: This method involved attaching two tendons to another angled pulley/shaft protruding from an 8mm one way needle roller bearing. The wheel could wind up tendons in one direction with the clutch bearing unengaged, then rotate the other way to engage the clutch bearing, and the string would slip from the angled inner shaft.

4) TPU flower-inspired compliant pulley: This method involved 3d printing a TPU pulley wheel with several compliant spokes. As the elastic potential stored up as the motor shortened the tendons, the torque experienced by the motor and pulley device increases, and so the spokes comply further. At a certain torque, the mutated angle of the spokes would cause the tendons to slide down and disengage from the pulley. The limitations of this method were that the system was difficult to tune and inconsistent. Similarly to section II-E.2, the tendons become contorted as they slip off.

5) Slip gearing: The selected and most successful mechanism was a 1:1 spur gear train where the driving gear is missing 8 teeth. The driving gear turned another with the pulley wheel connected to its shaft. The tendons are winded by the pulley, storing the elastic potential energy, and when the follower gear encounters the driver's section with no teeth, it disengages the pulley and lets it spin freely, releasing the built up elastic potential, and causing the buckling action. This system is good in comparison to the other methods because the tendons never become twisted. The limitations were inconsistency in the mechanism by virtue of the fingers having more than one resting state, and therefore the base length of the tendons changing.

F. Locomotion

As the bistable arms conform to the shape of the tree, the vertical tree was decided to be kept perpendicular to both arms so that they can wrap around it and provide hugging force as done in nature (in row A of figure 1). Perpendicularity was achieved using the gear train seen in figure 13 and by placing a single 180° servo motor in the center, a climbing gait was designed to constantly keep the bistable arms in the same orientation as the body moved.

To test the stability and payload capability of each claw, the robot was only built with two arms. High torque was required by the central servo motor as the fulcrum was the attachment point to the tree and for this reason the angle of the arms was changed to reduce the distance. An MG996R metal gear servo was selected to meet these torque requirements. Parts that were additively manufactured were produced with 15% infil to reduce the weight. Lego Technic pieces were used for the gearing as the strong ABS gear teeth are less subject to bending fatigue failure than additively manufactured or lasercut counterparts.

The robot was tested remotely, and controlled using two KY-023 Dual axis joystick modules for each set of tendons and a KY-040 Rotary Encoder to position the body servo.

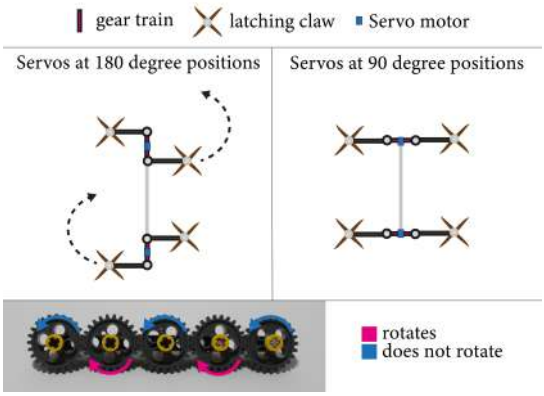

Fig. 13: Intended climbing gait design and relating gear configuration.

Fig. 14: Robot perching with both claws on Sessile oak tree.

Nrf24l01 modules at each endpoint let an Arduino Uno on the human's side communicates to an Arduino Nano on the robot's side. A 3.7v 2000mAh liPo battery was connected to a DC-DC boost converter to provide 5v to the three servo motors through extended 1.7Meter long wires. The battery was left off-board to reduce the weight of the robot in testing.

III. EXPERIMENTS & RESULTS

A. Finger Geometry Relationships

Tests were conducted to understand the relationship between the parameters that represent the 2D geometry of the bistable structure and their performance. It was observed during the build that a tapered bistable strip as a finger (with a narrower tip than base) required less pull force to reset. For this reason w_t, w_b and l, as illustrated in figure 7 were the variable parameters, and were measured against: the downwards force applied by the finger in state B, and the retraction force needed to reset the finger to stability state A. Each test geometry was produced symmetric about the centerline in the Y direction. Geometric measurements were accurate to $0.5mm$ and the strips were cut with fine point scissors. The bistable material used was from the Cieex slap bands for kids.

1) Activation measurements: The bistable finger unit was clamped above an AMIR Digital Scale with resolution to 0.01g, at a fixed height of 9mm and the downwards force that the bistable strip provided was measured. This measurement

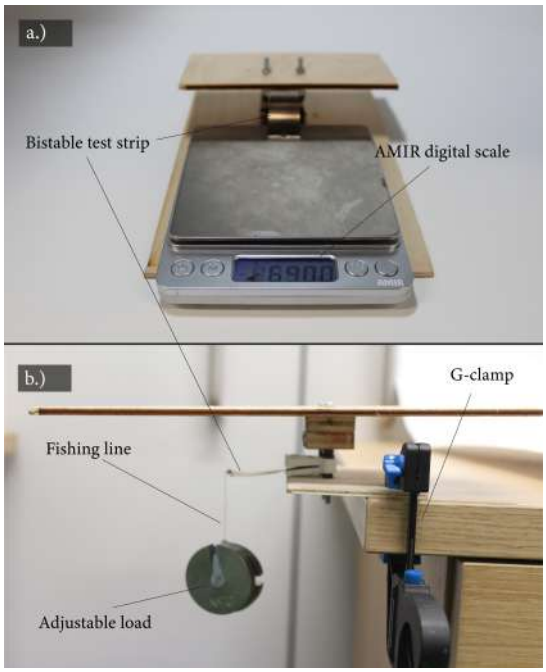

Fig. 15: Experimental setup: *a)* Measuring exertion forces *b)* Measuring retraction forces.

was converted to newtons, assuming gravitational acceleration as $9.81m/s$. For each test, the clamped section of the claw was kept parallel to the weighing scale and the force was exerted in the center of the scale each time, 18mm from back. The experimental setups are shown in *a)* of figure 15.

2) retraction measurements: The forces required for retraction from stability mode B back to mode A were measured by turning the setup upside down, clamping it to a table, and tieing weights to the tip of the bistable structures. A 2mm hole was drilled 3.5mm from the tip of the structure, and fishing line with a stopper knot was passed through it with weight attached to the other side. Continuous weight increments were added using Blu Tack for a resolution of 5g. Initial momentum was found to impact ease of retraction, so the weight was set from a 0 velocity position and left to do work on the system. The advantage of this method over using a dynamometer was that the weight always acted in the exact same direction.

3) Test one: varying length, l: The first test investigated the effect of varying the length of the bistable finger while keeping a constant width, where $w_t = w_b = 20mm$. Three measurements were taken for press force and were averaged.

4) Test two: varying width: The second test explored the effect of varying the width of the bistable structure, keeping the length constant, where $l = 30mm$, and $w_t = w_b$. Results for the first two experiments are displayed in figure 16.

5) Test three: varying taper: The third experiment tested the hypothesis mentioned in II-B.1 and measures the push force exerted and pullback force required for a range of tapers. Length is kept constant, where $l = 30mm$. Table I presents the raw data collected and figure 16 displays 3D scatter plots showing the relationship between w_b, w_t,

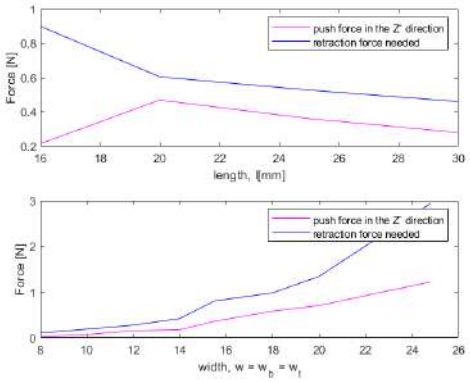

Fig. 16: Graph of results experiments one (top plot) and two (bottom plot).

exerted force and required retraction force respectively. The 'n/a' readings in the table represent where no amount of retraction force was able to reset the bistable strip. Rather than making this ∞, an arbitrary load value of 300g (or 2.93N) was chosen, so that the rest of the graph has a resolution which is interpretable.

$w_b[mm]$	w_t[mm]	press down weight [g]	Pullback weight[g]
24.8	24.8	124.2	n/a
24.8	20	111.62	177
24.8	16	106.58	127.1
24.8	12	101.44	94.66
24.8	8	94.75	88.24
20	24.8	124.2	n/a
20	20	111.62	177
20	16	106.58	127.1
20	12	101.44	94.66
20	8	94.75	88.24
16	24.8	124.2	n/a
16	20	111.62	177
16	16	106.58	127.1
16	12	101.44	94.66
16	8	94.75	88.24
12	24.8	124.2	n/a
12	20	111.62	177
12	16	106.58	127.1
12	12	101.44	94.66
12	8	94.75	88.24

TABLE I: Table presenting the raw data for experiment three - testing exertion and retraction forces for different tapering of the bistable strip.

Figure 18 exhibits the ratio of w_b/w_t against exerted and retraction forces. Further analysis was carried out to investigate whether there the surface area of the strip matches the forces exerted directly. The relationship is shown in figure 19. The area of each strip was calculated by taking the area of a trapezium $l/2(w_t + w_b)$ and summing the area of the remaining rectangle in the clawholder $16 * w_b$. The results of the three experiments are discussed in sections IV-B.

For reference, the bistable finger structure used in the latching claw design, whose dimensions are $l = 30mm$, $w_t = 8mm$, $w_b = 20mm$, had activation force of 37.5g from 9mm height and needed retraction force of 58g to

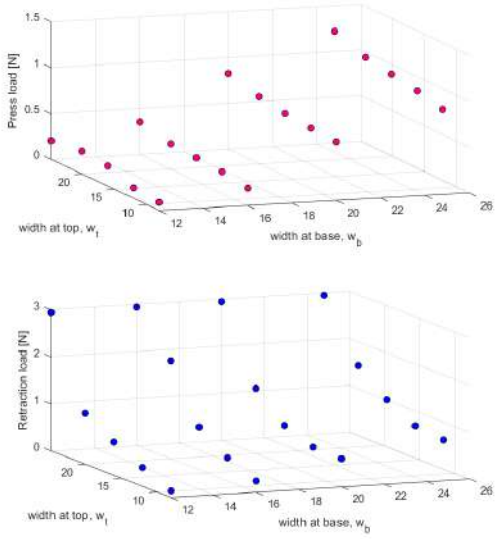

Fig. 17: 3D scatter plots of w_b vs w_t vs exertion force (top) or retraction force (bottom).

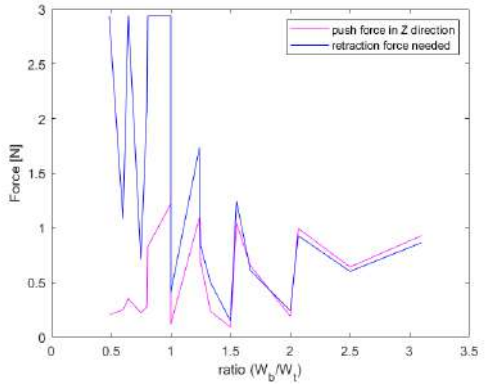

Fig. 18: Exertion forces and corresponding retraction forces for increasing ratios of w_b/w_t.

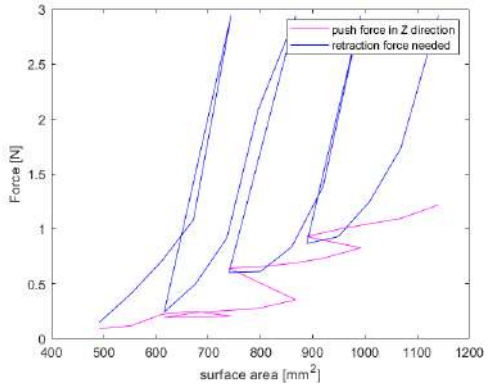

Fig. 19: Exertion forces and corresponding retraction forces plotted against 2D area of the bistable strip.

unlatch. Latching time was measured using the slow motion

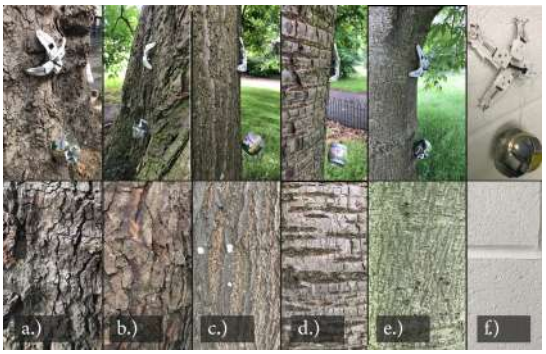

Fig. 20: Tree surfaces that were used for testing the clawed latching and payload performance.

recording function of the Iphone X which has resolution to 0.01s. The time difference was taken between the the finger unit contacting the latching surface and the bistable finger structure touching that surface. 5 videos were taken and the average time taken to deploy was 0.022 seconds.

B. Bistable Claw Performance

To augment the useful biomimetic characteristics that facilitate attaching to trees, the number of fingers on the claw were increased as seen in iteration 3 of figure 10. The claw was then able to reach more space on the tree and encounter patches of texture with more surface asperities, which was effective on Beech, Aspen, and grey Poplar. Increasing the number of fingers came at the cost of adding mass and requiring extra power to draw them back, but increasing the number of spines at the end of each finger had less detriment to the design.

Velcro achieves passive attachment through a large number of loop fasteners and compliant hooks. The contact force triggered latching described in this paper is already passive, and the following experiment looked to test whether rigid or compliant claw endings performed better in latching and gripping. Two types of 'glove' were designed to sheath the bistable finger strips.

3D printed spikes that covered the bottom were also considered, but the layer by layer manufacturing process meant that the tips were produced blunt. It was also observed that the bottom section of the claw rarely contacted the tree, unless the tree surface had low frequency textures (protruding lumps). This type of claw cover was therefore excluded from the performance testing.

1) galvanised sheet steel: Acuminate offcuts from the flexible steel naturally curled at the tip and their compliance varied depending on their width:length ratio. For each bistable finger structure, four cuts of base 3mm and height 4mm were melted in place between two 0.4mm sheets of PLA to form a spiked glove that was fastened to each finger.

2) Fishing hooks: The fishing hooks are sharp and rigid spines. Two were mounted symmetrically to either end of each finger at 90°.

The devices were placed face-on 10 times into arbitrary patches of the same tree. Both claws were tested in the same

place as each other on the tree. Five UK tree types of varying textures were tested, and can be seen in figure 20. An indoor concrete wall was also included in the analysis to understand if the design is well-situated and draw comparisons from the literature. The first time either claw latched and stayed stuck on the tree, the trial had begun and weight was attached to it on a string hanging 10mm from the base of the bottle cap. The weight was increased in 50g increments using a 1000 Gram Stainless Steel weight set. If the claw was unable to support 50g, the resolution was increased to 10g increments. The angle between the hanging string and the tree surface was measured digitally from a photo, therefore the resolution cannot be higher than 5°. On surfaces $\leq 90°$, the test weight holder would naturally lean against the tree; to ensure the test remained fair, the weight was manually swung outward. The claw itself weighs 24.08g with no payload. The main sources of weight are the M3 bolt PLA claw holder which weigh 4.45g combined. To make a fair test, the claw was placed on each test tree 10 times and the latching success rate was recorded. Success rates can be seen in table III.

		Compliant steel	Fishing Hooks
Surface Type	surface angle [○]	maximum weight[g]	maximum weight[g]
London Plane	$70 \leq \angle < 75$	300	>1000
	$90 \leq \angle < 95$	300	500
	$100 \leq \angle < 105$	150	600
Sessile Oak	$105 \leq \angle < 110$	400	700
	$65 \leq \angle < 70$	390	>1000
	$85 \leq \angle < 90$	450	>1000
Scarlet Oak	$85 \leq \angle < 90$	250	600
	$95 \leq \angle < 100$	400	>1000
	$90 \leq \angle < 95$	250	900
Wild Cherry	$95 \leq \angle < 100$	500	650
	$100 \leq \angle < 105$	500	>1000
	$85 \leq \angle < 90$	400	>1000
Sycamore	$88 \leq \angle < 93$	80	600
	$115 \leq \angle < 120$	130	650
	$85 \leq \angle < 90$	150	600
brick wall	90	190	400

TABLE II: Table showing the maximum weight that the claw was able to support after being latched to a random position of 5 tree types on the first try.

The results suggest that rigid fishing hooks are more effective at supporting payload and interlocking with surface asperities than the acuminate steel. The acuminate steel claw never surpasses 500g of payload, This could be the payload at which the compliant steel deforms and causes the robot to fall from the tree. The claw with just two fishing hooks consistently outperformed the other except for when latching onto concrete. The claw was also able to carry $> 1000g$ of payload with just two vertical fishing hooks engaged in the tree bark.

	compliant steel	Fishing Hooks
Surface Type	success rate [%]	success rate [%]
London Plane	100	100
Sessile Oak	100	100
Scarlet Oak	100	100
Wild Cherry	100	100
Sycamore	60	90
brick wall	30	10

TABLE III: Table displaying success rates for 10 attachment trials on the experimental tree surfaces.

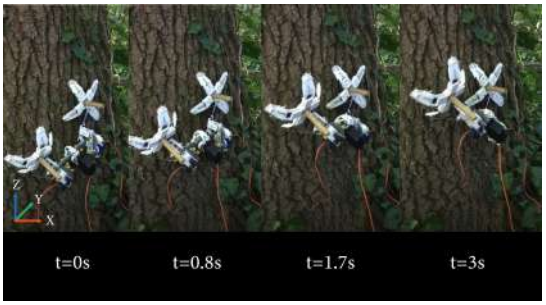

Fig. 21: Robot climbing - lifting arm motion shown over 3 seconds.

C. Robot climbing performance

As can be seen in figure 21, the robot described in section II-F had its climbing ability tested on dry Sessile Oak tree of diameter $> 50cm$. The robot weighed 224.3g and was able to perch on the tree and lift it's other arm. The weight of the body caused the bistable arm that was attached to the tree to bend backwards, and this meant that the lifting arm was not close enough to the tree to reattach. A spacer wheel was added in attempt to solve this problem but the arm was still too far out. The robot needs at least one extra rotational degree of freedom parallel to the y axis to guide the claw back to the tree.

IV. DISCUSSION

The results highlight the dependency on bark texture for gripping stability. As a general trend, the latching claw is more successful and consistent in supporting payload when the tree surface's texture has greater amplitude. This is likely to be because the surface asperities are deeper, and the spines can penetrate further in, increasing the vertical reaction force and hence supporting more weight (relating to the biological adaptation described in row B of figure 1).

A. Comparison to squirrels

Based on the results in table III, the discrepancy in gripping ability between squirrels (who will have a 100% success rate) and the latching claw could stem from their ability to use their sensory organs to coordinate their fingernail

positions directly into the miniature crevices. The latching claw design is probabilistic and relies on using a number of artificial fingernails to increase the chances of encountering surface asperities. The Amazon tropical rain-forest has over 918 different species of tree [20]. Even though the claw was successful on a variety of trees, bark infiltration provides more reliable gripping as it can ensure the biomimetic phenomenon by creating those asperities anywhere on the tree. The method is nonetheless constrained by the extra weight of the motors needed to undo that action. Bark penetration is easier when the bark is damp [10], therefore it should be explored as a rainforest-specific solution.

B. Experiments

The experiment described in section III-A investigated the relative effect of 2D material geometries on the force exerted, and retraction force needed to return to stability mode A.

1) Tests one and two: Both graphs in figure 16 clearly show that force exerted by the deployed bistable structure and the retraction force needed to reset the structure are correlated. The separation at the beginning of the varying length graph is expected to come from the bistable structure's length being too short to properly contact the scale. The width graph underneath shows that retraction force and force exerted become more similar at thinner widths of the bistable strcuture (when the bistable strip has less concave). This justifies greatly reducing the width of bistable structure used in the robot to increased efficiency.

2) Test three: The top scatter plot in figure 17 varies less significantly along the w_t axis than the w_b axis. Per contra, the scatter plot underneath it that describes retraction force diminishes significantly along the w_t axis. There is a drop in force $> 1.5N$ between $w_t = 20$ and $w_t = 12$ (points were taken directly from the curve). This affirms that reducing w_t compared to w_b and subsequently creating a taper improves the exerted force: retraction force ratio. Figure 18 also shows strong evidence that the taper had effect on the retraction force, as the ratio decreases, the required retraction force peaks. As the ratio increases, the retraction force becomes slightly less that that exerted. There is a general trend between surface area of the strip and force exerted by it. The experiment should be repeated to confirm or deny the oscillatory behaviour of the graphs in figures 18 and 19. This could have been caused by the limited accuracy of the experiment - in particular the geometry of the steel which was cut with scissors. If this behaviour were confirmed then the trend could be exploited to select taper ratios with lowest retraction force:exertion force ratios.

No research was conducted regarding which direction or stage of deployment the bistable strip produced force with largest magnitude. This could be tested by incrementally changing the angle or height at which bistable strip is positioned relative to the scale. The graphs that emerged from the experiment show retraction force as higher than exerted force. The force exerted was measured at a fixed height, which was unlikely to be that at which the bistables trip encounters the surface providing its peak force. The data was only collected to search for relationships between parameters.

3) Latching tests: The tree surfaces that were chosen for the tests had consistent texture and repeating patterns. The tests were limited nonetheless because the natural environment could not be controlled; even if a claw was placed on the tree multiple times in the same general area, it still may catch onto different surface asperities each time. Tree surfaces are mostly stochastic and so a high number of repeat tests are still needed to draw confident conclusions about their interaction with robots.

It was demonstrated through testing that adding anchors at the tip of each finger have greater effect on adhesive forces than increasing the compression force exerted by the gripper. The finger mechanisms in the latching claw move separately, although this could be advantageous, as each finger is able to conform to the irregular tree surface, this also means that there are different magnitudes of opposing force being exerted on the tree surface, depending on how curled the bistable structure is. There is no data yet to prove whether the claw would perform worse when all four fingers provide the same opposing force.

C. Robot Design

Perching robots like SCAMP use electronic actuators to engage microspines [17] and therefore cannot latch instantly. As a tradeoff, reversing the motor can disengage the microspines taking the exact same path back out. The tendon system used for the robot's latching claw cannot do this, and this is highlighted by the climbing test observations, as the robot's claw often became jammed. More compliant spines could be a potential solution (so that retracting the servo deforms the spines back out), but the latching claw tests suggest that compliance results in less payload, because heavy weight will deform the anchor points out of the asperities. Optimising the angle of tendon retraction to match that of the entry and remove the claw is another viable option to explore. The observation that the claw was able to support high payload with only the upward pointing fingers engaged could point us towards directional adhesion as another applicable solution. A gecko-inspired smooth vertical-surface climbing robot called Stickybot leverages directional adhesion easily to disengage from the surface it is attached to, by controlling tangential forces [21]. A similar phenomenon could be achieved in the tree climbing robot by running experiments whereby all the hooks on the fingers of facing downwards, and use a very particular paw retraction motion to detach with minimal effort. The servo motor retracted the four bistable fingers simultaneously. This meant that it had to overcome all four maxima of elastic potential energy in the same instance. Power consumption could be improved by designing a mechanism to stagger the retraction of each finger. The gait of the robot had low maneuverability, yet in a natural environment there are large amounts of variability, complexity and uncertainty. The robot needs more degrees of freedom to navigate uncertain settings;

Snakebot for example has lots of adaptability over limbed robots because of its high flexibility [22].

V. CONCLUSION & FUTURE WORK

Taking cues from squirrels and birds, a novel design is presented for lightweight, motorless, fast-latching bistable finger mechanisms deployed through surface contact force. The claw with rigid (non compliant) spines had most success attaching to trees and carrying heavy payloads. The heaviest payloads supported were on surfaces with furrowed tree bark and ridges. Deployment of the claw takes $0.2s$, while other vertical perching methods can take up to a second to engage [17] [23]. The claw responds passively to its interaction with the surrounding environment and has no reliance on sensory feedback to initiate latching. Other potential applications of the system could be catching fast moving objects.

The claw's separated finger mechanisms can individually conform to adapt to low frequency texture changes in the tree surface. Only omnidirectional finger configurations were tested in this paper to maximise the number of opposing spines [14]. Future work could explore the effects of arranging the fingers differently, for example using unidirectional configurations to create directional adhesion, and look to reduce the difficulty of retracting the claw from the tree. Bark textures are usually repeated with slight differences [24] and the most common patterns are vertical cracks; horizontal, outward-facing bistable fingers could therefore have been more appropriate and ought to be tested. Moving forward, the latching claw should be integrated into an aerial robot to test latching within the intended context.

Individual experiments have proven that by reducing the width of the bistable strip, the force that it exerts in a latched state becomes closer to the force needed to revert it back to its original state when pulling it back from the tip with a tendon.

The clawed device requires just one very lightweight motor to reset four fingers into an unlatched state. Motorised retraction had low success rate on trees that the claw was already attached to as the spines on the tip of each finger became stuck. The climbing robot that the claw design was integrated into was unable to take more than one step up the tree without human assistance due to it's inability to conform to the tree's shape. From an energy perspective the robot benefits from being underactuated, but more degrees of freedom are needed to climb complex and unpredictable environments.

REFERENCES

[1] M. J. Balunas and A. D. Kinghorn, "Drug discovery from medicinal plants," *Life Sciences*, vol. 78, no. 5, pp. 431–441, 2005, nATURECEUTICALS (NATURAL PRODUCTS), NUTRACEUTICALS, HERBAL BOTANICALS, AND PSYCHOACTIVES: DRUG DISCOVERY AND DRUG-DRUG INTERACTIONS. [Online]. Available: https://www.sciencedirect.com/science/article/pii/S0024320505008799

[2] N. Myers, "Tropical deforestation: the latest situation," *BioScience*, vol. 41, no. 5, pp. 282–283, 1991.

[3] S. Margulis, *Causes of deforestation of the Brazilian Amazon*. World Bank Publications, 2004, vol. 22.

[4] E. Richards, *Commercialization of non-timber forest products in Amazonia*. Natural Resources Institute, 1993, vol. 2.

[5] M. N. Faizal, W. Othman, and S. S. Hassan, "Development of pole-like tree climbing robot," in *2015 IEEE International Conference on Control System, Computing and Engineering (ICCSCE)*. IEEE, 2015, pp. 224–229.

[6] Y. Li, M. Z. Q. Chen, Y. H. Chen, and J. Lam, "Design of a one-motor tree-climbing robot," in *2015 IEEE International Conference on Information and Automation*, 2015, pp. 26–31.

[7] D. Ren, S. Yang, G. Yan, and Y. Zhang, "Study on a novel wheel type tree-climbing robot," in *2014 Seventh International Symposium on Computational Intelligence and Design*, vol. 1, 2014, pp. 150–153.

[8] G. C. Haynes, A. Khripin, G. Lynch, J. Amory, A. Saunders, A. A. Rizzi, and D. E. Koditschek, "Rapid pole climbing with a quadrupedal robot," in *2009 IEEE International Conference on Robotics and Automation*, 2009, pp. 2767–2772.

[9] T. L. Lam and Y. Xu, "Biologically inspired tree-climbing robot with continuum maneuvering mechanism," *Journal of Field Robotics*, vol. 29, no. 6, pp. 843–860, 2012.

[10] ——, "A flexible tree climbing robot: Treebot - design and implementation," in *2011 IEEE International Conference on Robotics and Automation*, 2011, pp. 5849–5854.

[11] M. Cartmill, *Chapter 5. Climbing*. Harvard University Press, 2013, pp. 73–88. [Online]. Available: https://doi.org/10.4159/harvard.9780674184404.c5

[12] D. A. Burnham, A. Feduccia, L. D. Martin, and A. R. Falk, "Tree climbing–a fundamental avian adaptation," *Journal of Systematic Palaeontology*, vol. 9, no. 1, pp. 103–107, 2011.

[13] W. R. T. Roderick, M. R. Cutkosky, and D. Lentink, "Bird-inspired dynamic grasping and perching in arboreal environments," *Science Robotics*, vol. 6, no. 61, p. eabj7562, 2021. [Online]. Available: https://www.science.org/doi/abs/10.1126/scirobotics.abj7562

[14] P. Chattopadhyay and S. K. Ghoshal, "Adhesion technologies of bio-inspired climbing robots: A survey," *International Journal of Robotics and Automation*, vol. 33, no. 6, 2018.

[15] A. T. Asbeck, S. Kim, A. McClung, A. Parness, and M. R. Cutkosky, "Climbing walls with microspines," in *IEEE ICRA*. Fla., 2006, pp. 4315–4317.

[16] A. Lussier Desbiens, A. T. Asbeck, and M. R. Cutkosky, "Landing, perching and taking off from vertical surfaces," *The International Journal of Robotics Research*, vol. 30, no. 3, pp. 355–370, 2011.

[17] M. T. Pope, C. W. Kimes, H. Jiang, E. W. Hawkes, M. A. Estrada, C. F. Kerst, W. R. Roderick, A. K. Han, D. L. Christensen, and M. R. Cutkosky, "A multimodal robot for perching and climbing on vertical outdoor surfaces," *IEEE Transactions on Robotics*, vol. 33, no. 1, pp. 38–48, 2016.

[18] Y. Cao, M. Derakhshani, Y. Fang, G. Huang, and C. Cao, "Bistable structures for advanced functional systems," *Advanced Functional Materials*, vol. 31, no. 45, p. 2106231, 2021.

[19] F. A. Kramer, "The activation energy of a slap bracelet," *Journal of Chemical Education*, vol. 70, no. 12, p. 1002, 1993.

[20] F. Wittmann, J. Schöngart, J. C. Montero, T. Motzer, W. J. Junk, M. T. Piedade, H. L. Queiroz, and M. Worbes, "Tree species composition and diversity gradients in white-water forests across the amazon basin," *Journal of biogeography*, vol. 33, no. 8, pp. 1334–1347, 2006.

[21] S. Kim, M. Spenko, S. Trujillo, B. Heyneman, D. Santos, and M. R. Cutkosky, "Smooth vertical surface climbing with directional adhesion," *IEEE Transactions on robotics*, vol. 24, no. 1, pp. 65–74, 2008.

[22] M. Nilsson, "Snake robot-free climbing," *IEEE Control Systems Magazine*, vol. 18, no. 1, pp. 21–26, 1998.

[23] A. Lussier Desbiens and M. R. Cutkosky, "Landing and perching on vertical surfaces with microspines for small unmanned air vehicles," *Journal of Intelligent and Robotic Systems*, vol. 57, no. 1, pp. 313–327, 2010.

[24] S. Fekri-Ershad, "Bark texture classification using improved local ternary patterns and multilayer neural network," *Expert Systems with Applications*, vol. 158, p. 113509, 2020. [Online]. Available: https://www.sciencedirect.com/science/article/pii/S095741742030333X